Mobile Direct Visualization of Pipes, Apexes, and Water Leaks in Water Distribution Networks

Jorge Luis Pérez Medina, Jean Vanderdonckt, Albéric De Coster and Sébastien Lambot

May 28, 2019

Mobile Direct Visualization of Pipes, Apexes, and Water Leaks in Water Distribution Networks

Jorge Luis Pérez Medina
Intelligent and Interactive Systems Lab (SI^2 Lab)
Universidad de Las Américas
Quito, ECUADOR
jorge.perez.medina@udla.edu.ec

Jean Vanderdonckt
Université catholique de Louvain (UCL)
LouRIM - Place des Doyens, 1 – B-1348
Louvain-la-neuve, BELGIUM
jean.vanderdonckt@uclouvain.be

Albéric De Coster
Université catholique de Louvain (UCL)
Earth and Life Institute - Croix du Sud, 2 – B-1348
Louvain-la-neuve, BELGIUM
alberic.decoster@uclouvain.be

Sébastien Lambot
Université catholique de Louvain (UCL)
Earth and Life Institute - Croix du Sud, 2 – B-1348
Louvain-la-neuve, BELGIUM
sebastien.lambot@uclouvain.be

***Abstract*—Technological innovations, such as Ground-Penetrating Radar (GPR) provide a non-destructive and non-invasive solution to support the processes of detection of water leaks in water distribution networks. SENSPORT is an initiative funded by the Walloon Region in Belgium. The purpose of the project was to use a Ground-Penetrating Radar in conjunction with intelligent and embedded systems to provide a feasible, low cost and non-invasive solution. We introduce the value in detecting water leaks on roads and underground pipes in cities. This contribution presents an agile development life cycle to obtain the human-computer interface in a mobile device e.g., tablet-like) to visualize water leaks in an area being studied. The visualization mechanisms that have been used contemplate the data processing as images and 2D/3D representations on mobile devices.**

***Index Terms*—Ground-penetrating radar (GPR), Information Visualization, Mobile user interface, Radar data visualization, water leak detection, water leakage, water management.**

I. INTRODUCTION

More than half (54%) of the world's human population resides in the cities and this number is expected to reach 66% by 2050 as a result of the high rates of urbanization in developing countries [1]. Urbanization brings with it the implementation of different public services, such as: health, transport, electricity and water distribution networks. One of the great current challenges is the efficient and effective management of such services. Efficient management involves the maximum use of all the resources that are necessary to optimize the quality of the services.

Water leaks detection in the supply networks is an important task because the losses generally reach 20-30% of the total production. These references can be increased up to 50% in the oldest distribution networks [2]–[5]. Water leaks can lead to public health problems. While the lower the pressure in the water supply systems, greater is the possibility of contaminant intrusions [6], [7]. Moreover, water leaks is the origin of economic losses loss that includes the cost of the raw water, its treatment and its transportation. It have also an unfavorable impact of natural resource conservation. In addition, they also lead to financial losses as they are the origin of erosion around the pipes, damages to buildings, road foundations [8] and supply disruptions.

Several technological advances, academic and industrial, have been taken into account to detect water leaks in supply distribution networks. The use of a particular method depends on the conditions where it must be applied. State of the art reviews of the existing techniques used to detect water leaks, including devices and equipment are available in [6], [9]–[11]. Once a potential leak is identified, tools can be used to obtain more accurately the affected area. Ground-penetrating radar (GPR) appears to be a non-invasive and non-destructive alternative [12]. It technology can be used to capture high-resolution datasets in order to reproduce 3D images of the subsoil. "Fig. 1" illustrates an example of interactive visualization of water leaks in a mobile device from data recovered from the subsoil. Water distribution companies can analyze the exact location of a water leak before conducting exploratory excavations. As a consequence, the mechanism saves resources and time in the management and treatment of water distribution networks. The principle of this geophysical technique consists in transmitting electromagnetic waves into the medium and recording the signal backscattered by the dielectric contrasts originating from the presence of underground layers or buried utilities. GPR offers a significant advantage compared to other techniques used for leaks detection. Its benefit is to differentiate the underground structures. This discrimination allows to recognize the pipes, allowing in this way to reduce the excavation area. By reducing the excavation area, operating costs are reduced, as well as the risks associated with collateral damage (breaking other cables, pipes...).

Ensuring a good interpretation of GPR data makes it necessary to study and put into operation an image processing strategy. Consequently, it is necessary to design a mobile,

Fig. 1. interactive visualization of water leaks in a mobile device.

light, simple and intuitive interface that guarantees the visualization of the data in a three-dimensional space. The aim of this contribution is to propose a user-friendly visualization interface to in order to make easy the interpretation of Ground-Penetrating Radar data required by leak detection process when is applied to water distribution networks. Development makes use of a user-centered approach described in [13], where the user interface is one of the most important elements of development. The efficiency and effectiveness of a friendly user interface (UI) to visualize GPR-based radar data can be influenced by different factors: the user interface, the interaction of the user with the application and/or the quality of the contained information. Considering these factor, the purpose of this contribution is to presents the detail in the design and development of a smart user strategy to visualize 2D/3D radar data. The user interface developed becomes a feasible alternative in the process to detect and monitor water leaks. The contribution is structured as follows: section 2, we describe the fundamental ideas of the SENSPORT project in which we have studied a GPR radar data visualization strategy. Section 3 describes the details of the conception of a mobile interface to support the visualization, interpretation and detection of leaks in water distribution networks. Section 4 presents some discussions. Finally, conclusions and some observations for future work are presented.

II. SENSPORT

The innovative SENSPORT project was conducted under the financial support of the Walloon Region, in Belgium. This project aimed at developing GPR capabilities to detecting leaks in supply water distribution services and to provide detailed information about underground structures in a non-destructive way. The proposed method of SENSPORT was presented in [8]. The presented method consists of obtaining information from the subsoil through the use of antennas in order to supporting the detection of water leaks with the help of detection algorithms and segmentation of the reflections obtained. The process involves techniques of quantitative estimation of the properties of the elements found in the study area through full-wave inversion. One of the scopes of SENSPORT is to offer a new end-user interface developed to visualize 3-D radar data and display the detected objects on mobile devices. SENSPORT has been the subject of several studies that have involved laboratory experiments as part of proof of concept [8].

Details of the SENSPORT methodology to detect leaks and pipes is presented in [8]. The first step which is currently semi-automated, consists in acquiring parallel GPR profiles above the place where the presence of a leak is suspected. The radar data, which are provided in a specific format by the GPR manufacturer, are subsequently read and saved in a .mat format using a commercial software package (MATLAB R2014a, The MathWorks Inc.). After having obtained the raw GPR data, a qualitative imaging processing is performed to allows the detection of the objects presented in the subsoil area. Next, we filtering the multiple internal reflections of the antenna and their ringing of the GPR data captured, considering the near-field circumstances. Subsequently, the objects present in the subsoil (for instance, stones, pipes...) and the layers are identified by using the filtered GPR cross-sections data on their precise marks. The GPR data processed in a three-dimensional format allows us to detect a series of hyperbolas. The hyperbolas allow us to identify the pipes. The process consists of identifying the candidate hyperbolas, by connecting all the connected components within a cross section. It process is a well-known technique and its details are presented in [14].

A visualization user interface obtain the coordinates of the pipes and the apexes identified in order to facilitates the interpretation of the information. We also incorporate a color scale to offer a degree of reliability of the detection process. It represents a way to inform final users of the probability of detecting pipes and vertices. The communication between the object detection algorithm and the visualization interface is achieved through JSON files. This kind of format was selected because of its compatibility with Web applications. A structure that includes the 3D signal amplitude matrix and the three vectors containing the graduations for the three dimensions are then sent to the visualization application. It makes the end-user able to visualize the 2D and 3D GPR raw data in order to facilitate a previous interpretation of the studied area in real time.

The proposed visualization interface supporting the usage of mobile devices and conventional computer. It supports water leak visualization and their interpretation. The functionalities of the visualization GPR interface are as follows:

1) *Show plan*: the interface of visualization should allow the visualization of a plan. The Plan is the principal area of visualization. on this area the application show all the images along the cross-sections (or XZ space), the depth-slices (or XY space) and the perpendicular sections (or YZ space).
2) *Show views*: it area allows to operate the scene of the visualization user interface. The operator can consult the different views of the scene. it consists of fixing the views according to different directions (for instance, Top and Bottom, Front and Back...) and also allowing the realization of adjustments and rotations.
3) *Move Image according to Axis*: the operator must have the possibility to manipulate the images, pointed by the final user, according to the axes: X, Y and Z. It allows to show one particular image according to the Position (or the X axis), the Transect (or the Y axis) and the Depth (or the Z axis).

4) *Show Edge*: the operator must have to show the edges or borders of the displayed images in order to visualize the pipes. The operator must configure their most adequate view of the edges of each image by using a threshold component. Additional filter like brightness, saturation and others can be used to facilitate a better manipulation of the images.
5) *Show the map*: the operator can view the map contained the location where the GPR data was captured.
6) *Show Pipes, Apexes and Floor*: the operator can activate or hide the visualization of the vertices and the pipes detected by the algorithms. Also, the operator can use a probability threshold to obtain a view of the apexes and pipes according to probability values. The visualization interface assigns a probability color for each detected pipe or apex.
7) *Create a report*: the operator can download a report contained the scene as an image, including a short description.

III. HUMAN-COMPUTER INTERFACE AND VISUALIZATION

The human-computer interface of SENSPORT is a user-friendly mobile application that offers final-users the functionalities to visualize and interpret unprocessed/processed GPR radar data like as "the pipe(s)" and the probability of water leak in a 2D/3D viewing scene.

A. Development of the visualization tool

This section focuses on the end-user interface developed to visualize the 3D GPR data. This visualization tool is a multi-device and multi-platform application designed to help the end-user to determine the position of the pipe(s) and to detect the presence of a suspected water leak. Three tasks have to be carried out to ensure the appropriateness of the application: (1) the identification of the user requirements and the modeling of the use context; (2) the design process for the development of a 2D/3D data visualization strategy facilitating the interpretation of the data; and (3) the iterative user-friendly prototyping supporting multi device and multi platform contexts.

1) The identification of the user requirements: The usability goals, user characteristics and problem context were diagnosed and analyzed through a flexible Collaborative User Centered Design method [13]. This multi-stage problem-solving procedure was used because it allows an effective and flexible communication between all the actors involved at the beginning of an iterative process of development of any interactive system, when it is essential to capture the functional and technical needs of the application. In parallel with the user needs diagnosis, a task model was created and complemented with several sketches of the user interface. An abstract interface was then derived from these information and was afterwards converted into a concrete interface. These steps were guided using the Cameleon framework [15]. This framework constitutes an important reference model for classifying user interfaces, supporting the study of multiple user's contexts or multiple targets in the domain area of context-aware computing.

2) Modeling of the use context: Early, in the design phase of the visualization application SENSPORT, different interfaces and visualization techniques were specified, developed or prototyped. "Fig. 2" shows different interfaces as a result of an iterative process of re-design and optimization of the human-computer visualization system. The visualization of the GPR data was the main task achieved during the conception and optimization of the ergonomic human-machine interface. It assists the operator in displaying the processed data in three dimensions using an interface offering all the functionalities needed to process and interpret the data. It means that the final user should get information about the data pointed out by the cursor and should be able to scroll and zoom in order to obtain more detailed information. We used data acquired in laboratory conditions to implement and assess the 3-D visualization functionalities.

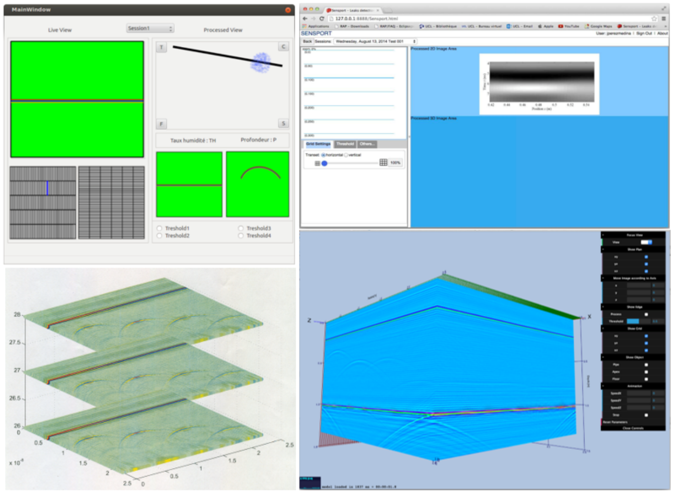

Fig. 2. Iterative Design of Direct Visualization Interface.

The first step achieved to create the visualization tool consisted in looking for different data visualization frameworks and selecting those adapted to the developed interface considering the user's requirements. The criteria considered in the framework selection procedure were the compatibility with the Web technology and the ability of the framework to be supported by various devices and cross-platform mobile applications. With respect to the SENSPORT project, the following solutions were in particular investigated: D3[1], HighchartsJS[2] and ThreeJS[3]. The tests achieved to assess the capabilities of the three libraries with respect to radar data visualization showed the inappropriateness of the HighchartsJS and D3 libraries. The first two tests were conducted using the D3 and

---

[1] http://d3js.org/ D3 is a JavaScript library used to manipulate documents based on data.

[2] http://www.highcharts.com/ Highcharts js is a JavaScript charting library that use Vector Markup Language (VML) rendering and Scalable Vector Graphics (SVG).

[3] http://threejs.org/ Three.js is a cross-browser JavaScript library/API that makes WebGL 3-D easy to use in modern browsers.

HighchartsJS libraries. Our purpose was to show the raw GPR data in a 3D. we incorporated a color attributed in function of the radar data amplitude.

“Fig. 3” shows the result of the test performed using the D3 library. We find that the execution time increases when the number of displayed points is greater. Our tests indicate that for visualizing 12.801 points the execution time is 1.32 seconds, which constitutes an inappropriate time response according to the requirements. In general, the number of points regarding GPR surveys is huge (e.g., a water leak survey contains about 1 million points on an area of 9-10m2), which prevents the time response to fulfill the requirements.

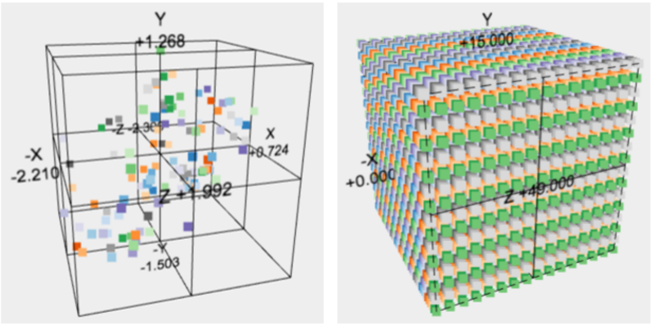

Visualization of 129 points

Visualization of 12.801 points - **1.32 seconds**

Fig. 3. Results of the test performed using the D3 library.

Similarly, we performed the same experiment using the HighchartJS library (see “Fig. 4”) and we obtained again bad performance regarding the time required to visualize the radar data. Indeed, about 396 ms were needed to load a model made of 999 points. HighchartJS is even less adapted as it does not display the data if the number of points is superior to 999. Therefore, with the aim of decreasing the execution time needed to display radar data, we decided to use the JavaScript ThreeJS framework in order to visualize the GPR data as a representation of images (.png format) instead of points. The aim was the significant decrease of the execution time needed to display the radar data.

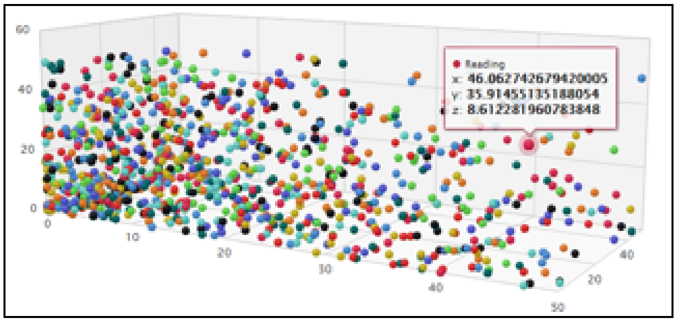

Fig. 4. Results of the test performed using the HighchartJS library.

The radar system is a mobile device sending electromagnetic waves into the medium. The backscattered signals or A-scans are then sampled and can be gathered to provide an image also called B-scan. If several B-scans are acquired in parallel above a specific area, a C-scan (= 3-D image) can be generated by appending them. The distance between the B-scans depends on the required resolution (operator decision), the frequency band of the antenna and the field conditions. Realistic distances can be implemented in the 3-D visualization interface but it is often easier to interpret data when the B-scans are close to each other. Therefore, we defined a distance factor that reduces virtually the distance between B-scans. During the transformation process, we had to apply a pseudo color scheme to represent the contrasts generated by the amplitude differences. The choice of the scheme is important as some of them give a better rendering of the contrasts and enhance data visualization. “Fig. 5” shows several examples when applying pseudo color schemes to images.

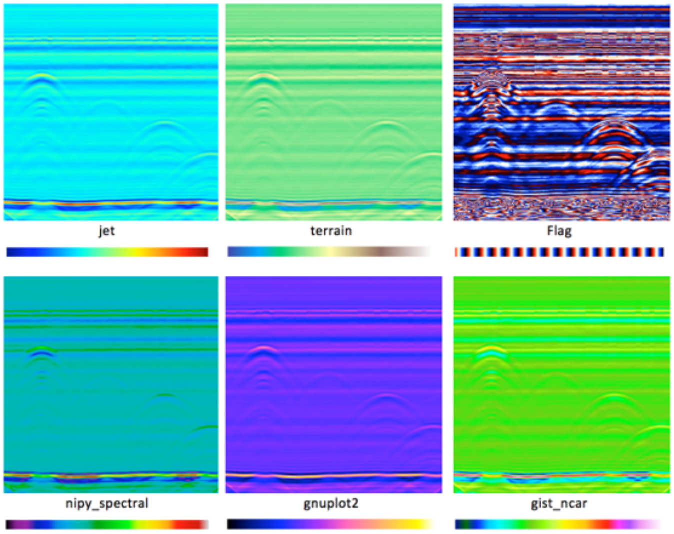

Fig. 5. Applying pseudo color schemes to the images.

We decided to use the Jet pseudo color scheme for the visualization with Three.js as that scheme highlighted the contrasts in an adapted way in Matlab. Fig. 6 (panel a) shows a processed B-scan/radar image, (panel b) shows an example of 3D visualization for five processed GPR slices, respectively.

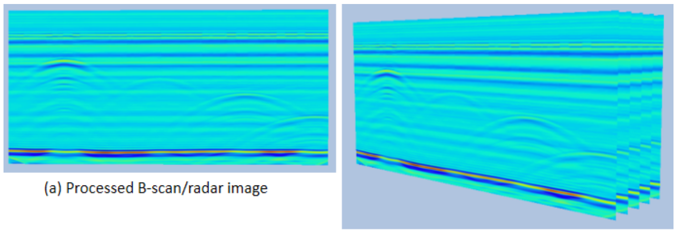

(a) Processed B-scan/radar image

(b) An example of 3D visualization for five processed GPR slices

Fig. 6. 3D representation using as reference images radar.

B. The data acquisition process

Fig. 7 illustrates a semi-automated procedure to cover the whole processing chain. Raw data reading with Mathlab (3D matrix containing the amplitude values and three vectors for each dimension).

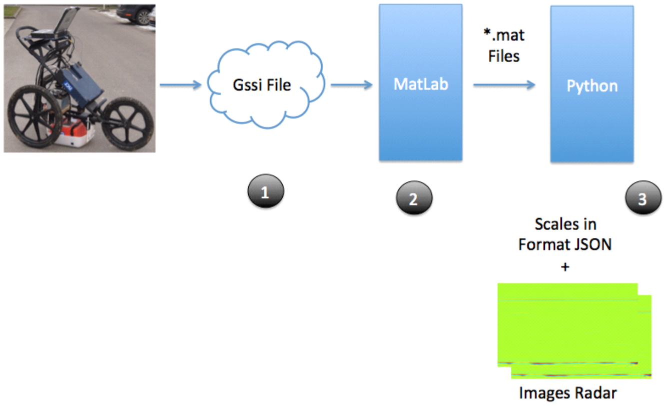

Fig. 7. The data acquisition process.

The Python language was used to transform the radar data into images that are subsequently displayed in the visualization tool. Several libraries peculiar to this language were used to achieve this goal. The Scipy[4] library, a Python-based ecosystem for mathematics, sciences and engineering, was used to convert 3-D datasets from Matlab into 3-D Python matrices. These matrices can subsequently be processed with the Python Imaging Library[5] to generate radar images having X, Y and Z axes. As a reminder, these axes represent the position along the profile, the transect number and the propagation time/depth, respectively. The scales of the three axes were stored in a JSON file. The use of the multiprocessing Python package[6] was necessary to parallelize the generation of the GPR images and, thereby, to improve the performance of the transformation of the Matlab data into .png radar images.

C. *GPR data visualization interface*

For the human-computer interface of SENSPORT, showing all the GPR data on small screens was a big challenge, not only regarding the limited screen resolution, but also due to limited computational performances, including the graphic card. In order to tackle this issue, we made use of the 2D Starfield visualization technique proposed by [16]. As complement, we developed a 3D galaxy based display technique for reduced screens (e.g., in order to be manipulated on a powerful smartphone or tablet). We also resort to the proposal of Burigat (2009) [17] that highlights the way of coupling large amounts of data with access functionalities, making it easier for the user to explore large amounts of data. This principle exploits direct operation functionalities such as aligning the view to a coordinate and the perspectives of specific three-dimensional planes to take advantage of the limited surfaces offered by the screens of mobile devices. Based on these considerations, we designed a visualization interface aiming at offering to the user the greatest flexibility in the exploration of the data. The capability of the User Interface to support concurrently a general overview and data details is an approach that has been typical for information visualization. The experimental results, presented in [18], affirm that this visualization strategy is effective to reduce the completion time of tasks in a reasonable range of operation. They also ensure an adequate satisfaction perception of the users when manipulating reduced surfaces. End-users have a greater preference for maintain the contextual overview fully, while manipulating a a set of data (unlike a simplified zoom user interface).

The 3D radar data visualization interface showed in “Fig. 8” was achieved using the Three.js library.

The visualization user interface is structured according to the following components: (1) the scene; (2) the menu and (3) the area where the data was captured. The last element permits to identify the precise location indicating where the survey was conducted and could later be part of a geographic information application. A more detailed description of some elements and functionalities can be found hereinafter.

1) The scene: “Fig. 8” shows an example of the scene that includes the radar images located in the XYZ system of coordinates. The XZ (red), YZ (green) and XY (blue) planes allow displaying the transects (cross-sections), the GPR slices perpendicular to the acquired transects and the plan views of the data at a designated depth (also called z-slices), respectively. A specific measuring scale is computed for each axis.

2) The functionalities of the menu: Final users can manipulate the scene by using the menu of functionalities. The main functionalities were carried out according to the specifications described in section II on page 2. Additionally, we have made the following options:

1) Setting colors: it allows you to assign a particular color to each density index. The probabilities to show the existence of pipes are expressed by 3 ranges.The ranges are defined as follows: [0-25%], [25-75%], [75-100%]
2) Animation: it allows to the user to activate and/or deactivate an automatic movement of the images for the 3 axis X, Y and Z. The movements begin with the first image. When the final image is reached, it returns to the initial image. The user can also indicate the speed of movement for each axis. In case of 0 the animation is stopped for the associated axis
3) Headtracking: it option allows to activate and/or deactivate face’s detection of the final user in order to permit an interaction with the visualization interface by augmented web gestures. The interaction allows slightly changing the rotation/orientation of the images, for example: vertical and horizontal movements

Is worth noticing that some features are linked to mechanisms that allow to detect the edges of the images whereas some others focus on objects (pipes ...) visualization. The processes implemented to achieve these tasks require the use of different algorithms and are explained in the following sections.

3) Image filter analyses: Image filtering techniques can be used in to improve the preliminary analysis of the raw GPR data. Several image filtering strategies have been studied with

---

[4] http://www.scipy.org/

[5] http://www.pythonware.com/products/pil/

[6] https://docs.python.org/dev/library/multiprocessing.html

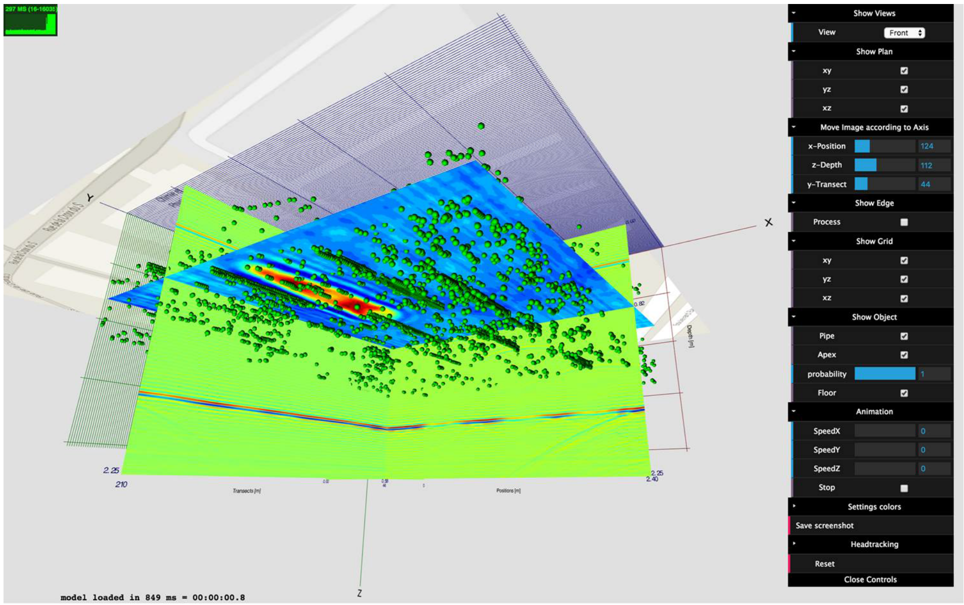

Show Views
View Front
Show Plan
xy ☑
yz ☑
xz ☑
Move Image according to Axis
x-Position 124
z-Depth 112
y-Transect 44
Show Edge
Process ☐
Show Grid
xy ☑
yz ☑
xz ☑
Show Object
Pipe ☑
Apex ☑
probability 1
Floor ☑
Animation
SpeedX 0
SpeedY 0
SpeedZ 0
Stop ☐
Settings colors
Save screenshot
Headtracking
Reset
Close Controls

```
model loaded in 849 ms = 00:00:00.8
```

Fig. 8. The final visualization interface.

respect to the computation time required to be activated and applied on 3-D radar images.

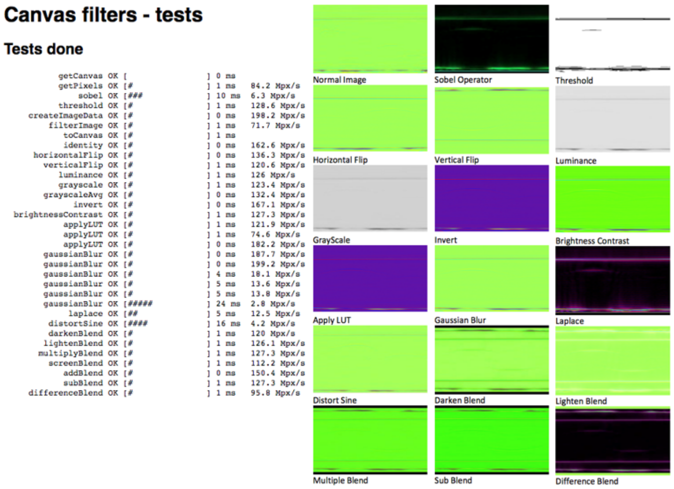

Canvas filters - tests

Tests done

```
           getCanvas OK [                ] 0 ms
           getPixels OK [#               ] 1 ms    84.2 Mpx/s
               sobel OK [###             ] 10 ms   6.3 Mpx/s
           threshold OK [#               ] 1 ms    128.6 Mpx/s
     createImageData OK [#               ] 0 ms    198.2 Mpx/s
         filterImage OK [#               ] 1 ms    71.7 Mpx/s
            toCanvas OK [#               ] 1 ms
            identity OK [#               ] 0 ms    162.6 Mpx/s
      horizontalFlip OK [#               ] 0 ms    136.3 Mpx/s
        verticalFlip OK [#               ] 1 ms    120.6 Mpx/s
           luminance OK [#               ] 1 ms    126 Mpx/s
           grayscale OK [#               ] 1 ms    123.4 Mpx/s
        grayscaleAvg OK [#               ] 0 ms    132.4 Mpx/s
              invert OK [#               ] 0 ms    167.1 Mpx/s
  brightnessContrast OK [#               ] 1 ms    127.3 Mpx/s
            applyLUT OK [#               ] 1 ms    121.9 Mpx/s
            applyLUT OK [#               ] 1 ms    74.6 Mpx/s
            applyLUT OK [#               ] 0 ms    182.2 Mpx/s
        gaussianBlur OK [#               ] 0 ms    187.7 Mpx/s
        gaussianBlur OK [#               ] 0 ms    199.2 Mpx/s
        gaussianBlur OK [#               ] 4 ms    18.1 Mpx/s
        gaussianBlur OK [#               ] 5 ms    13.6 Mpx/s
        gaussianBlur OK [#               ] 5 ms    13.8 Mpx/s
        gaussianBlur OK [#####           ] 24 ms   2.8 Mpx/s
             laplace OK [##              ] 5 ms    12.5 Mpx/s
          distortSine OK [####           ] 16 ms   4.2 Mpx/s
          darkenBlend OK [#              ] 1 ms    120 Mpx/s
        lightenBlend OK [#               ] 1 ms    126.1 Mpx/s
       multiplyBlend OK [#               ] 1 ms    127.3 Mpx/s
         screenBlend OK [#               ] 1 ms    112.2 Mpx/s
            addBlend OK [#               ] 0 ms    150.4 Mpx/s
            subBlend OK [#               ] 1 ms    127.3 Mpx/s
     differenceBlend OK [#               ] 1 ms    95.8 Mpx/s
```

Fig. 9. Applying image filter to the processed B-scan/radar image.

Fig. 9 shows several results when applying different filters on processed B-scan/radar image. User can processing the images by using the threshold. It consists in the substitution of the pixels having an intensity lower or greater than a reference value by a null/transparent value. However, this offers a total vision of the contrasts that the totality of the data must have. Therefore, we decided to first process the produced images with the Sobel operator [19], [20]. We also analyzed the computation time required to activate the threshold and apply the functionality on 3D radar images. The results showed in Fig. 9 evidences that applying a Sobel operator to an image requires 21 milliseconds while the Threshold technique only requires 1 millisecond. However, even if it demands a less important processing time, the latter does not provide a good view of the contrasts that the other parts of the data have. Therefore, we decided to focus mainly on the Sobel operator and the Frei-Chen edge detector algorithm [21]. These techniques were selected because they provided a better and efficient detection of the edges and contrasts during the radar image processing.

Fig. 10 (panel b) shows an example of the threshold processing step using the Sobel operator. It is worth noting that four hyperbolas were detected in this picture. Despite their higher processing time, these filtering techniques give a greater detection of contrasts and also the edges for the images. The edge detector algorithm called “Frei-Chen” offers similar performances to those highlighted for the Sobel operator and provides a slightly better edge detection quality (see “Fig. 10”, panel c). For each pixel, we applied a threshold criterion and a threshold inversion procedure similar to those used with the Sobel operator. “Frei-Chen” is more efficient because the algorithm uses principally a factor of normalization, and several techniques to exclude the features that are not edges. Thus, the “Frei-Chen” seems to have a better functioning because it is more efficient against noisy data and its behavior is better, than the Sobel operator, in situations where it is necessary to detect edges created by small gradient. However, “Frei-Chen” and Sobel were in incorporated into the visualization interface because the Frei-Chen edge detector has a more important computational cost.

We suggest studying other recent techniques in order to incorporate them as an alternative to hyperbolas detection. In addition to the previous threshold operator, different complementary tools can be used to help visualizing and interpreting the subsoil. They were implemented in the new interface as advanced parameters that can be modified by the user. We performed additional tests with these tools to improve the detection of the edges. These tests combined other techniques for filtering images. The filtering techniques used are: Invert,

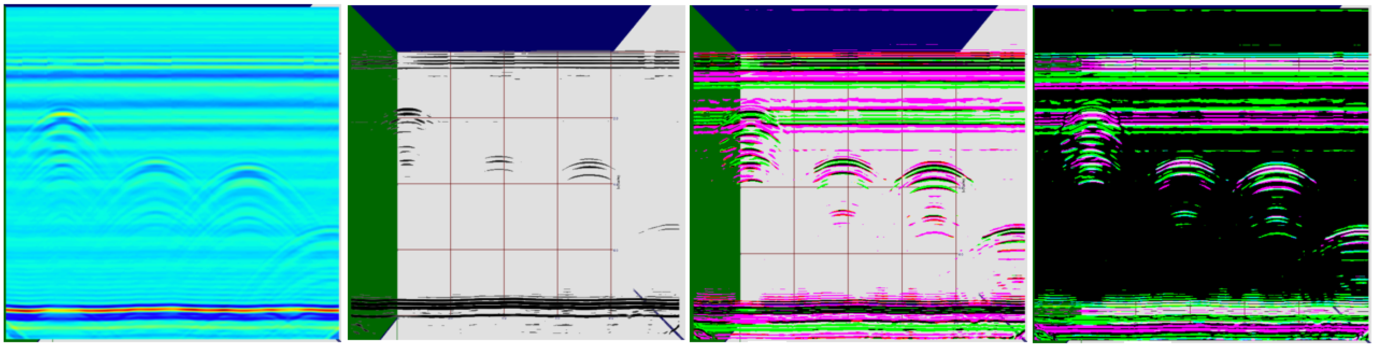

(a) Original image (b) Sobel algorithm (c) Frei-Chen filter (d) Invert

Fig. 10. Applying image filter to the processed B-scan/radar image.

Brightness, Hue, Saturation and Value (HSV) and Posterize. The Invert technique replaces black pixels by white and vice versa. This operation is achieved by subtracting each of the RGB pixel values from 1.0. “Fig. 10” (panel d) shows an example of the technique applied to a radar image.

The brightness modification allows producing lighter or darker images by adding or subtracting a constant to all the RGB pixels values. As a reminder, the RGB model is represented by amplitude ranges of brilliance varying from 0% to 100% of red, green and blue for a particular color. The ranges of values are represented in WebGL by decimal numbers ranging from 0 to 255 or by their corresponding hexadecimal number from 00 to FF.

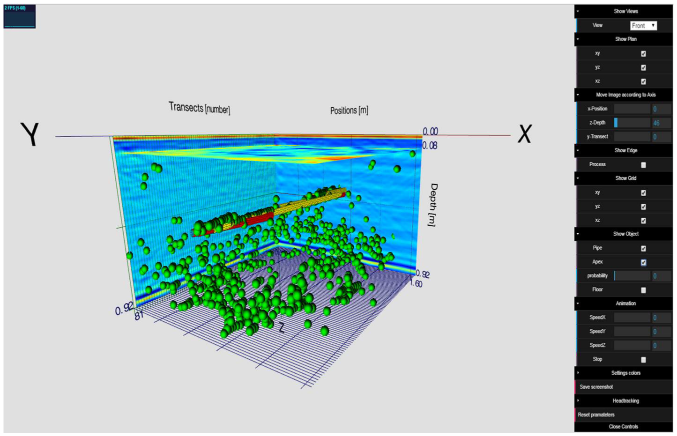

Fig. 11. The Human-computer interface to 3D GPR data visualization.

The manipulation of Hue, Saturation and Value (HSV) of color pixels can improve the appearance of images regarding RGB pixels values. Hue indicates the visual color sensation of the light. It represents the degree for a stimulus described as different or similar according to the stimuli produced by the perceived colors: blue, green, red and yellow. The saturation corresponds to the purity or intensity of a hue. If the saturation increases, the colors appear purer while, in counterpart, the colors look more ”decolorized” if its value decreases. When we conduct the classification of the pixels of an image in the RGB system, the saturation, the value and the hue are stored in the green, blue and red channel respectively. The aim of the HSV manipulation consists in removing shadows and separating the color components in terms of intensity in order to obtain robustness against lighting changes. The posterization of an image is a process dividing the continuous gradation of color tone into several regions of fewer tones while maintaining a semblance of the original image characteristics. The reduction of the number of colors in the image is made possible by quantizing the RGB levels of each pixel. The number of bins or regions required for each channel can be specified before processing the image. The posterization allows detecting the lines of contours.

4) The representation of pipes and apexes: The human-computer D visualization interface allows the final-user to see the pipes and vertices recognized in the scene. The information transferred to the interface through the JSON file includes the three coordinates. The interface also allows to visualize estimates of the approximate obtained permittivity of the area neighboring the pipes, and also the apex density indicator. This probability index, represents a reliability value associated to the pipes detection. “Fig. 11” shows the integration of the detected apexes and pipes in the human-computer 3D visualization interface. Based on the density value of the index, the end-user can augmented/reduce the presence of apexes and pipes. Finally, the density value of the index is defined by a color scale.

IV. GENERAL DISCUSSIONS

SENSPORT project is a conscious initiative that aims to offer a set of techniques that allow efficient detection leaks in water supply distribution networks. Its foundation is the processing of Ground-Penetrating Radar data capture in the area where the presence of a leak is estimated. Several quantitative techniques are used for the purpose of analyze the captured raw GPR data of the subsoil and thus make an accurate estimation of the underground elements, like as: cables, stones, pipes, etc.

A human-computer 3D visualization interface was designed through an agile approach centered on the end-user, as a support to the visualization and interpretation of the GPR data. This interface has the goodness of running on devices with small screens. The technique for presenting the data consists of transforming the radar data into images according to three axes. Quantitative data analysis was also carried out in order to estimate the relative permittivity. In this way we got the water content around a pipe.

Different preliminary studies were conducted in the installations of the Georadar Research Center of the Université catholique de Louvain[7] to validate the proposed solution [8]. The experiment allowed us to demonstrate the proof of concept by capturing near-field values on a leaking pipe. The pipe was buried in a medium composed of sand. The results are acceptable. They evidence the importance of processing GPR data, making a visualization in three dimensions and considering the results of a quantitative processing from the GPR data inversions [8]. By capturing a three-dimensional dataset we were able to recognize continuous objects, that is, the pipes, cables, stones and also other point-like objects presented in the studied area. These detections do not allow to restrict the explorations of water leaks in smaller selected areas, but also, they allow us to know which are the positions of the closest structures in order to avoid damaging the excavations.

V. CONCLUSION

For societies it is not a secret that water leaks represent a problem in terms of conservation of natural resources, economic losses, financial losses due to interruptions in the supply of the service. From another perspective, water leaks represent damage to buildings and public roads. SENSPORT intends to offer a non-destructive alternative strategy that supports the detection and management of water leaks with economy of resources and time. In this paper, we proposed a novel mobile human-computer interface supporting the interpretation of GPR data radar in a 3D display space. The solution contemplates imagery and visualization techniques. The process of construction of the interface was carried out through an iterative process. Therefore, future efforts should consider the quantitative reconstruction of GPR data captured in heterogeneous area. Likewise, We consider to include additional information about the water content in the visualization interface. Finally, we plan to validate the work carried out in several conditions like as, road and highway.

ACKNOWLEDGMENT

This contribution was financed by the Walloon Region by SENSPORT project (Convention no1217720) through the WBGreen program. We also received the support of the Fonds National de la Recherche Scientifique of Belgium (FNRS-Belgium) and also the COST TU1208 Action, financed by the European Union: “Civil Engineering Applications of the Terrain Penetration Radar”.

REFERENCES

[1] U. Nations, “World population prospects: The 2015 revision,” *United Nations Econ Soc Aff*, vol. 33, no. 2, pp. 1–66, 2015.

[2] M. Charlton and M. Mulligan, “Efficient detection of mains water leaks using ground-penetrating radar (GPR),” in *Subsurface and Surface Sensing Technologies and Applications III*, vol. 4491. International Society for Optics and Photonics, 2001, pp. 375–387.

[3] L. C. Cheong, “Unaccounted for water and the economics of leak detection,” in *Proc. International Water Supply Congress and Exhibition, Copenhagen. Water Supply*, vol. 9, 1991.

[4] A. F. Colombo and B. W. Karney, “Energy and costs of leaky pipes: toward comprehensive picture,” *Journal of Water Resources Planning and Management*, vol. 128, no. 6, pp. 441–450, 2002.

[5] N. N. Halimshah, A. Yusup, Z. M. Amin, and M. D. Ghazalli, “Visual Inspection of Water Leakage from Ground Penetrating Radar Radargram,” *ISPRS Annals of the Photogrammetry, Remote Sensing and Spatial Information Sciences*, vol. 2, no. 2, p. 191, 2015.

[6] O. Hunaidi, W. Chu, A. Wang, and W. Guan, “Detecting leaks in plastic pipes,” *Journal-American Water Works Association*, vol. 92, no. 2, pp. 82–94, 2000.

[7] P. Rizzo, “Water and wastewater pipe nondestructive evaluation and health monitoring: a review,” *Advances in Civil Engineering*, vol. 2010, 2010.

[8] A. D. Coster, J. Pérez-Medina, M. Nottebaere, K. Alkhalifeh, X. Neyt, J. Vanderdonckt, and S. Lambot, “Towards an improvement of GPR-based detection of pipes and leaks in water distribution networks,” *Journal of Applied Geophysics*, 2019. [Online]. Available: http://www.sciencedirect.com/science/article/pii/S0926985117310790

[9] T. Hao, C. Rogers, N. Metje, D. Chapman, J. Muggleton, K. Foo, P. Wang, S. R. Pennock, P. Atkins, S. Swingler *et al.*, “Condition assessment of the buried utility service infrastructure,” *Tunnelling and Underground Space Technology*, vol. 28, pp. 331–344, 2012.

[10] Z. Liu and Y. Kleiner, “State of the art review of inspection technologies for condition assessment of water pipes,” *Measurement*, vol. 46, no. 1, pp. 1–15, 2013.

[11] R. Puust, Z. Kapelan, D. Savic, and T. Koppel, “A review of methods for leakage management in pipe networks,” *Urban Water Journal*, vol. 7, no. 1, pp. 25–45, 2010.

[12] A. Cataldo, R. Persico, G. Leucci, E. De Benedetto, G. Cannazza, L. Matera, and L. De Giorgi, “Time domain reflectometry, ground penetrating radar and electrical resistivity tomography: a comparative analysis of alternative approaches for leak detection in underground pipes,” *NDT & E International*, vol. 62, pp. 14–28, 2014.

[13] J. L. Pérez-Medina and J. Vanderdonckt, “Sketching by Cross-Surface Collaboration,” in *Information Technology and Systems*, Á. Rocha, C. Ferrás, and M. Paredes, Eds. Cham: Springer International Publishing, 2019, pp. 386–397.

[14] M. Ardekani, P. Druyts, S. Lambot, A. De Coster, and X. Neyt, “Recovering the structure of a layered soil, including layer thickness and dielectric permittivity, using the interfaces and objects backscatter detected in GPR B-scans,” in *Ground Penetrating Radar (GPR), 2014 15th International Conference on*. IEEE, 2014, pp. 397–400.

[15] G. Calvary, J. Coutaz, D. Thevenin, Q. Limbourg, L. Bouillon, and J. Vanderdonckt, “A Unifying Reference Framework for multi-target user interfaces,” *Interacting with computers*, vol. 15, no. 3, pp. 289–308, 2003.

[16] C. Ahlberg and B. Shneiderman, “Visual information seeking: Tight coupling of dynamic query filters with starfield displays,” in *The Craft of Information Visualization*. Elsevier, 2003, pp. 7–13.

[17] S. Burigat and L. Chittaro, “A mobile starfield visualization with space compression capabilities,” in *Proceedings of the 11th International Conference on Human-Computer Interaction with Mobile Devices and Services*. ACM, 2009, p. 81.

[18] T. Buering, J. Gerken, and H. Reiterer, “User interaction with scatterplots on small screens-a comparative evaluation of geometric-semantic zoom and fisheye distortion,” *IEEE Transactions on Visualization & Computer Graphics*, no. 5, pp. 829–836, 2006.

[19] N. Kanopoulos, N. Vasanthavada, and R. L. Baker, “Design of an image edge detection filter using the Sobel operator,” *IEEE Journal of solid-state circuits*, vol. 23, no. 2, pp. 358–367, 1988.

[20] O. R. Vincent and O. Folorunso, “A descriptive algorithm for Sobel image edge detection,” in *Proceedings of Informing Science & IT Education Conference (InSITE)*, vol. 40. Informing Science Institute California, 2009, pp. 97–107.

[21] R.-H. Park, “A Fourier interpretation of the Frei-chen edge masks,” *Pattern Recognition Letters*, vol. 11, no. 9, pp. 631–636, 1990.

---

[7] http://sites.uclouvain.be/gprlouvain